Acta Crystallographica Section F
Structural Biology and Crystallization Communications
ISSN 1744-3091

Fast high-pressure freezing of protein crystals in their mother liquor

Anja Burkhardt,[a]*‡ Martin Warmer,[b]‡ Saravanan Panneerselvam,[a] Armin Wagner,[c] Athina Zouni,[d] Carina Glöckner,[d] Rudolph Reimer,[b] Heinrich Hohenberg[b] and Alke Meents[a]

[a]Deutsches Elektronen-Synchrotron DESY, Notkestrasse 85, 22607 Hamburg, Germany, [b]Heinrich-Pette-Institute, Leibniz Institute for Experimental Virology, Martinistrasse 52, 20251 Hamburg, Germany, [c]Diamond Light Source, Chilton, Didcot, Oxfordshire OX11 0DE, England, and [d]Max-Volmer-Laboratory for Biophysical Chemistry and Biochemistry, Technical University Berlin, Strasse des 17. Juni 135, 10623 Berlin, Germany

‡ These authors contributed equally to this work.

Correspondence e-mail: anja.burkhardt@desy.de.

Received 1 February 2012
Accepted 5 March 2012

PDB References: HEWL flash-cooled at high pressure, 4a7d; porcine insulin flash-cooled at high pressure, 4a7e.

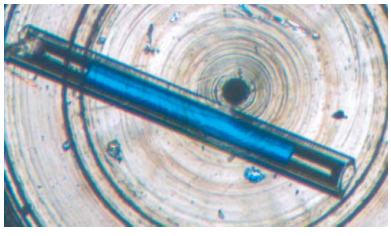

High-pressure freezing (HPF) is a method which allows sample vitrification without cryoprotectants. In the present work, protein crystals were cooled to cryogenic temperatures at a pressure of 210 MPa. In contrast to other HPF methods published to date in the field of cryocrystallography, this protocol involves rapid sample cooling using a standard HPF device. The fast cooling rates allow HPF of protein crystals directly in their mother liquor without the need for cryoprotectants or external reagents. HPF was first attempted with hen egg-white lysozyme and cubic insulin crystals, yielding good to excellent diffraction quality. Non-cryoprotected crystals of the membrane protein photosystem II have been successfully cryocooled for the first time. This indicates that the presented HPF method is well suited to the vitrification of challenging systems with large unit cells and weak crystal contacts.

1. Introduction

Flash-cooling to cryogenic temperatures is the standard method of reducing X-ray-induced radiation damage to protein crystals during data collection (Garman & Schneider, 1997; Garman & Owen, 2006; Rodgers, 1994; Meents *et al.*, 2010). Cryocooling usually requires considerable concentrations of cryoprotectants, such as glycerol or ethylene glycol, in order to prevent the formation of hexagonal ice upon cooling. Finding ideal cryoconditions can be very time-consuming and challenging, in particular for large-unit-cell systems such as membrane proteins or viruses. Moreover, the crystal quality is often degraded upon cryoprotection, which limits the quality of the diffraction data.

In the field of electron microscopy (EM), large biological objects such as cells or tissue are typically vitrified by high-pressure freezing (HPF; Moor, 1971; Hohenberg *et al.*, 1994; Studer *et al.*, 1995, 2008). Similar to many macromolecular crystals, biological samples possess a large amount of solvent which can be converted into high-density amorphous (HDA) ice by freezing at high pressures without the use of cryoprotectants.

In cryocrystallography, HPF has been applied to many different proteins of medium molecular weight and unit-cell size (Thomanek *et al.*, 1973; Kim *et al.*, 2005). Details of HPF experiments conducted in the field of macromolecular crystallography are summarized in Table 1. Although the method of Kim *et al.* (2005) is available to users at the macromolecular diffraction facility at CHESS (Englich *et al.*, 2011), successful HPF has not yet been reported for membrane proteins or viruses with only weak crystal contacts.

In both published methods for HPF in the field of cryocrystallography, the mother liquor has to be removed from the crystal surface. The crystals are either immersed in 2-methylbutane (Thomanek *et al.*, 1973) or coated with NVH oil (Cargille immersion oil, type NVH, viscosity 21 000 $mm^2 s^{-1}$; Kim *et al.*, 2005) in order to prevent crystal dehydration during pressurization. NVH oil may additionally act as a nonpenetrative (external) cryoprotectant. After the pressure has been slowly raised to a few hundred megapascals at room temperature, the whole pressure vessel is plunged into liquid nitrogen. The

Table 1
Overview of HPF of protein crystals.

Protein	Crystallization conditions	Cryoprotectant	External reagent	*p* (MPa)	Cooling rate (K s^{-1})	Solvent content (%)	Unit-cell volume (10^5 Å^3)	Resolution limit (Å)	Reference
Sperm whale myoglobin	3.75 *M* $(NH_4)_2SO_4$	None	2-Methylbutane	250	2	†	†	2.2	Thomanek *et al.* (1973)
Sperm whale myoglobin	72–78% $(NH_4)_2SO_4$, pH 5.5–6.0	None	2-Methylbutane	150–200	1.7	35	6.54	1.7	Urayama *et al.* (2002)
Glucose isomerase	1.15 *M* $(NH_4)_2SO_4$, 1 m*M* $MgSO_4$, 10 m*M* HEPES, pH 7.5	None	NVH oil	130	1.7‡	55	9.41	1.3	Kim *et al.* (2005)
Thaumatin	0.9 *M* disodium tartrate, 50 m*M* HEPES, pH 7.0	None	NVH oil	185	1.7‡	57	5.08	1.9	Kim *et al.* (2005)
AHP-LAAO	2 *M* $(NH_4)_2SO_4$, 0.1 *M* trisodium citrate, pH 5.0	None	NVH oil	190	1.7‡	62	47.33	2.7	Kim *et al.* (2005)
RNase A	0.1 *M* sodium acetate, 30% $(NH_4)_2SO_4$, 50% NaCl, pH 6.0	10% glycerol	None	180–200	1.7‡	61	2.24	2.0	Chen *et al.* (2009)
Porcine pancreatic elastase	30 m*M* $(NH_4)_2SO_4$, 50 m*M* sodium acetate, pH 5.0	None	NVH oil	155	1.7‡	35	1.98	1.3	Kim *et al.* (2006)
Citrine	50 m*M* sodium acetate, 50 m*M* ammonium acetate, 5% PEG 3350, pH 5.0	None	NVH oil	200	1.7‡	42	2.30	1.8	Barstow *et al.* (2008)
Carbonic anhydrase II	1.3 *M* trisodium citrate, 100 m*M* Tris–HCl, pH 7.8	20% glycerol	NVH oil	1.5	1.7‡	38	1.24	1.1	Domsic *et al.* (2008)
Hen egg-white lysozyme	0.1 *M* sodium acetate, 15% NaCl, pH 4.6	None	None	210	7000§	36¶	2.21¶	1.4¶	This work
Porcine insulin	0.5 *M* NaH_2PO_4, 0.01 *M* EDTA, pH 10.0	None	None	210	7000§	62¶	4.63¶	1.9¶	This work
Photosystem II	100 m*M* PIPES, 5 m*M* $CaCl_2$, 0.015% *N*-β-dodecyl maltoside, 3.5–4.5% PEG 2000, pH 7.0	None	None	210	7000§	64††	92.35	4.5	This work

† Not available. ‡ Cooling rates taken from Urayama *et al.* (2002). § Cooling rates taken from Shimoni & Müller (1998). ¶ Data given for the best data set. †† According to Guskov *et al.* (2009).

maximum cooling rates reached at the sample surface are therefore relatively low at 1–2 K s^{-1} (Kim *et al.*, 2005; Urayama *et al.*, 2002).

In contrast, surface cooling rates in the range of 3×10^3–2×10^4 K s^{-1} are required to vitrify biological samples at 210 MPa (Riehle, 1968; Bald, 1986). Thus, an instrument providing fast cooling rates would be preferable for HPF of sensitive crystals.

The goal of this work was to determine whether standard EM protocols and equipment can be used for HPF of protein crystals. It was further intended to test whether this HPF protocol can also be applied to large-unit-cell systems such as a membrane protein. Tetragonal hen egg-white lysozyme (tHEWL) and cubic porcine insulin were chosen as initial model systems. tHEWL crystals contain a low amount of solvent (39.5%; Vaney *et al.*, 1996) and can be flash-cooled without cryoprotectants. Cubic insulin crystals have a higher solvent content (65.2%; Gursky *et al.*, 1992) and require the application of cryoprotectants upon flash-cooling (Nanao *et al.*, 2005; Meents *et al.*, 2007; Yu & Caspar, 1998). In addition, the light-harvesting protein photosystem II (PSII) was chosen as a representative of a membrane protein with a large unit cell. PSII crystals have a solvent content of 64% (Guskov *et al.*, 2009) and a unit-cell volume of 92.35×10^5 Å^3 (this work). In general, finding optimal cryoconditions for large-unit-cell systems with weak crystal contacts is very challenging. Such crystals easily exhibit physical damage (such as cracking) owing to osmotic shock when soaked in a solution of different ionic strength. Moreover, crystals with unit cells in excess of 400 Å usually have weak crystal contacts and are therefore very fragile and difficult to handle (Fry *et al.*, 2007). PSII crystals usually require the application of a stepwise cryoprotection protocol with a final concentration of 25–30% glycerol for data collection at cryogenic temperatures. Such glycerol-cryoprotected PSII crystals diffracted to a resolution of 1.9 Å (Umena *et al.*, 2011) or 2.9 Å (Guskov *et al.*, 2009) and showed an average mosaicity of 0.2–0.3° (Kern, Loll, Zouni *et al.*, 2005). In contrast to conventional flash-cooling with cryoprotectants, HPF does not require such a time-consuming cryoprotection procedure. Here, the crystals can be directly frozen in their mother liquor without the use of cryoprotectants.

2. Experimental

2.1. Protein crystallization

Tetragonal crystals of hen egg-white lysozyme (tHEWL; Sigma–Aldrich, catalogue No. L-6876) were directly grown in quartz capillaries (length 80 mm, outer diameter 100 µm, wall thickness 10–20 µm) at 298 K using the gel-acupuncture method [García-Ruiz & Moreno, 1994; Otálora *et al.*, 1996; 50 mg ml^{-1} tHEWL in 0.1 *M* sodium acetate buffer pH 4.6; 15%(*w*/*v*) NaCl in 0.1 *M* sodium acetate buffer pH 4.6]. tHEWL crystals filling the inner diameter of the quartz capillary (60–80 µm) were obtained after 5 d. The length of the crystals varied between 60 and 1200 µm.

Cubic Zn-free insulin crystals were grown by hanging-drop vapour diffusion by mixing 3 µl 15 mg ml^{-1} porcine insulin (Sigma–Aldrich, catalogue No. I-5523) solution in 0.05 *M* sodium phosphate buffer pH 10.0, 0.01 *M* EDTA with 3 µl 0.5 *M* sodium phosphate buffer pH 10.0, 0.01 *M* EDTA. The mixture was equilibrated against 500 µl 0.5 *M* sodium phosphate buffer pH 10.0, 0.01 *M* EDTA at 298 K. Single crystals between $50 \times 50 \times 50$ and $70 \times 70 \times 70$ µm in size were selected for HPF experiments under a stereo microscope.

PSII was crystallized as reported previously (Kern, Loll, Lüneberg *et al.*, 2005), but was not cryoprotected with glycerol. A PSII crystal with estimated dimensions of $600 \times 300 \times 120$ µm was selected for HPF.

2.2. Sample preparation

Two HPF methods involving a Baltec HPM 010 high-pressure freezer are presented in this paper. Method *A* was used for HPF of tHEWL and cubic insulin crystals in quartz capillaries. Method *B* was used for PSII as it allows HPF of larger crystals which are known to diffract to higher resolution. In method *B* the crystals can be directly frozen in their crystallization buffer without 1-hexadecene.

2.2.1. Method *A*. Quartz capillaries were purchased from Müller & Müller OHG, Germany [length 80 mm, outer diameter 100 µm (tHEWL) or 200 µm (cubic insulin), wall thickness 10–20 µm]. The crystals were either directly grown in quartz capillaries (tHEWL) or

were soaked into them (cubic insulin) using a hydraulic piston pump (CellTram vario, Eppendorf AG). Quartz capillaries containing the crystals and their mother liquor were immediately submerged in 1-hexadecene. The capillaries, which were initially 80 mm in length, were cut under a stereo microscope into segments of a maximum length of 2 mm using a diamond-coated razor blade (DIAMAZE). Each segment contained only one protein crystal and was completely filled with mother liquor (see Fig. 1). The cutting was performed under 1-hexadecene to prevent evaporation of the mother liquor. Owing to its hydrophobicity 1-hexadecene is not soluble in water and the crystals are protected against dehydration without affecting the composition of the mother liquor. As shown in Fig. 2, the capillary segments were transferred to an aluminium platelet with a cavity of a diameter of 2 mm and a depth of 150 µm for tHEWL and 200 µm for cubic insulin. The cavity was filled with 1-hexadecene, which was used as a freezing medium in order to improve the heat transfer from the sample to the aluminium platelet. The platelet containing the capillary segment was subsequently sandwiched with a second platelet (lid), which was oriented so that its planar surface was facing the sample.

2.2.2. Method *B*. PSII sample preparation was entirely carried out under green light. The PSII crystal was transferred to a Teflon platelet using a LithoLoop (Molecular Dimensions). The Teflon platelet was prepared by gluing a 170 µm thick Teflon ring with an outer diameter of 3 mm and an inner diameter of 2 mm on top of a 8 µm thick Kapton foil with a diameter of 3 mm. Thus, a platelet with a 170 µm deep cavity was obtained, which was filled with crystallization buffer containing 8% PEG 2000. After transfer of the PSII crystal the Teflon platelet was covered with a second Kapton foil (see Fig. 2). For HPF the Teflon platelet was finally sandwiched between the planar surfaces of two aluminium lids.

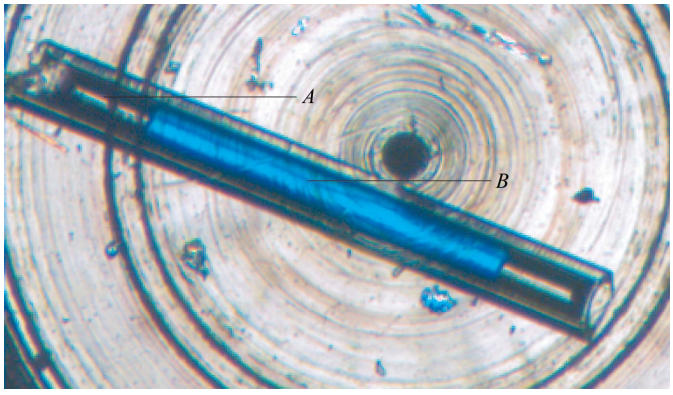

Figure 1
A tHEWL crystal in a quartz capillary submerged in 1-hexadecene (picture taken under a polarizing microscope): *A*, mother liquor; *B*, tHEWL crystal.

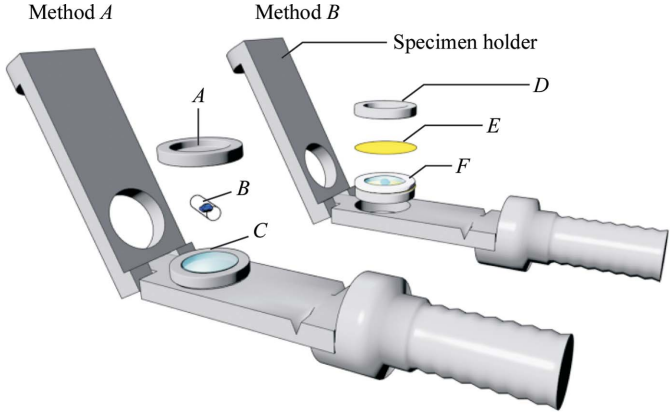

Figure 2
Sample preparation for HPF. Method *A* (front): *A*, aluminium lid; *B*, quartz capillary containing the crystal in its mother liquor; *C*, aluminium platelet with cavity filled with 1-hexadecene. The sample is sandwiched between the platelet and the lid under 1-hexadecene and is then transferred to the specimen holder. Method *B* (back): *D*, aluminium lid; *E*, Kapton foil; *F*, Teflon platelet containing the crystal in its crystallization buffer. Sample preparation is performed in the specimen holder, which is subsequently inserted into the HPF device.

2.3. High-pressure freezing procedure

The protein crystals were subjected to HPF according to a procedure used for the vitrification of biological samples (Hohenberg *et al.*, 1994). HPF was carried out at 210 MPa and 77 K using a Baltec (formerly known as Balzers) HPM 010 instrument, which is shown in Fig. 3. The principle of this HPF device has been described in detail by Dahl & Staehelin (1989). In brief, the sample sandwiched between the aluminium platelets is transferred to the specimen holder (see Fig. 2) and inserted into the HPF device. Subsequently, ethanol is automatically injected at room temperature and completely fills the pressure chamber containing the sample. Immediately after ethanol injection, liquid nitrogen pressurized to 210 MPa is 'shot' onto the specimen holder *via* a jet. The compressibility of ethanol (κ = 1.1 GPa^{-1}) at 274 K is similar to that of water (κ = 0.5 GPa^{-1}; Dorfmüller *et al.*, 1998). Owing to the low compressibility of ethanol, the pressure is directly transferred to the crystal. Thus, a pressure of 210 MPa is attained in the pressure chamber within 20 ms. The ethanol surrounding the aluminium platelets is substituted by liquid nitrogen, which rapidly cools the sample to 77 K. Using this procedure, cooling rates of about 7000 K s^{-1} are obtained at the sample surface (Shimoni & Müller, 1998). This HPF procedure guarantees that the sample is at a pressure of 210 MPa before the sample is cooled below 273 K. After HPF the samples are instantaneously transferred to liquid nitrogen, removed from the HPF specimen holder and stored at 77 K until further use.

2.4. Sample manipulation after HPF

2.4.1. Method *A*. The tHEWL and cubic insulin samples were transferred to a reservoir of 2-methylbutane located in a conventional freeze substitution system (AFS2, Leica Microsystems, Austria) which was adjusted to 135 K in order to prevent the formation of hexagonal ice. The capillary segments were removed from the aluminium platelets and lids. Extraneous frozen 1-hexadecene

Figure 3
Baltec HPM 010 high-pressure freezing device.

Table 2
Summary of data-collection parameters for HPF crystals of tHEWL, cubic insulin and PSII.

	HPF tHEWL	HPF cubic insulin	HPF PSII
Beamline	I04-1	X06DA	I24
Wavelength (Å)	0.9163	0.9253	0.9686
Oscillation range (°)	0.2	0.5	0.2
Exposure time (s)	0.2	3	0.2
Crystal-to-detector distance (mm)	152	150	450
Beam dimensions ($h \times v$) (µm)	60 × 50	80 × 45	10 × 10
No. of images	1800	180	100

Table 3
Data-set statistics for HPF crystals of tHEWL and cubic insulin.

The first value in each column is the average value over all data sets. The following values in parentheses are the lowest and the highest values found within the corresponding group. Overall data-set statistics are given for resolution ranges of 50.0–2.0 Å for HPF tHEWL and 50.0–1.85 Å for HPF cubic insulin.

	HPF tHEWL	HPF cubic insulin
Space group	$P4_32_12$	$I2_13$
Unit-cell parameters (Å)	a = 77.94 (76.78, 78.85), c = 37.25 (36.81, 37.55)	a = 77.31 (77.28, 77.35)
Unit-cell volume (Å^3)	226341 (217001, 233087)	462010 (461531, 462787)
Resolution limit (Å)	1.78 (1.44, 2.43)	1.86 (1.85, 1.87)
R_{merge}, overall (%)	4.9 (2.6, 8.0)	6.4 (5.5, 7.4)
Completeness, overall (%)	99.3 (95.5, 99.8)	99.6 (99.4, 99.7)
$\langle I/\sigma(I)\rangle$, overall	21.16 (11.67, 34.16)	18.89 (17.05, 19.98)
Multiplicity, overall	20.4 (16.3, 24.5)	9.3 (9.2, 9.4)
R_{merge}, 2.5–2.0 Å (%)	8.4 (4.0, 13.2)	11.9 (10.8, 13.6)
Completeness, 2.5–2.0 Å (%)	99.4 (94.9, 100.0)	99.9 (99.8, 100.0)
$\langle I/\sigma(I)\rangle$, 2.5–2.0 Å	13.08 (6.47, 24.54)	9.63 (8.26, 10.56)
Wilson B factor (Å^2)	24.9 (21.7, 29.5)	33.6 (31.6, 37.4)
Mosaicity (°)	0.45 (0.14, 0.99)	0.09 (0.09, 0.10)
No. of crystals	10	3

(boiling point 547 K, melting point 275 K) was scraped off using a scalpel. Adhering 2-methylbutane was removed from the capillary surfaces with pre-cooled filter paper. The capillary segments were subsequently glued onto a nylon loop (Hampton Research) using cryoglue (2:3 ethanol:2-propanol) at 135 K. The capillaries were mounted in such a way that their longest dimension was oriented perpendicular to the X-ray beam. Samples were stored at 77 K until diffraction experiments were performed. Particular care was taken to keep the samples at cryogenic temperatures during shipping and mounting at the beamline.

2.4.2. Method *B*. The Teflon ring containing the HPF PSII crystal in its crystallization buffer was removed from both aluminium lids using a razor blade at 77 K. The Teflon ring was mounted on a home-made brass clamp for data collection and was stored at 77 K.

2.5. Data collection, data processing and structure refinement

Diffraction data for tHEWL and PSII were collected at the undulator beamline I04-1 and the microfocus beamline I24 at Diamond Light Source, Didcot, England, respectively. Diffraction data for cubic insulin were collected at the super-bending-magnet beamline X06DA (PXIII) at the Swiss Light Source, Villigen, Switzerland. Data sets were collected at ambient pressure (0.1 MPa) and 100 K using an open-flow nitrogen cryostat. Detailed information on the data-collection parameters are summarized in Table 2.

All data were processed using the *XDS* program package (Kabsch, 2010). The unit-cell parameters and crystal mosaicity of each data set were determined during the *XDS* refinement process. Data-set statistics for HPF tHEWL and HPF cubic insulin were calculated with *XSCALE* (Kabsch, 2010) and are given in Table 3. The resolution limit was defined as the resolution shell that still provided a completeness of 50% at $I/\sigma(I) \geq 2$ (Sheldrick *et al.*, 1993). To obtain an indicator of the absolute crystal quality, all data were scaled with a resolution limit of 2.0 Å for tHEWL and 1.85 Å for cubic insulin. To indicate the quality of the high-resolution data, resolution shells of 2.5–2.0 Å were chosen for both proteins.

Table 4
Structure-refinement parameters for HPF tHEWL and HPF cubic insulin.

R_{free} is the R value calculated from 5% of the data that were randomly chosen and omitted from refinement.

	HPF tHEWL	HPF cubic insulin
R_{work}	0.175	0.176
R_{free}	0.203	0.217
R.m.s. deviation from ideality		
Bond lengths (Å)	0.007	0.015
Angles (°)	1.039	1.510

The best data sets from HPF tHEWL and cubic insulin were used for structure refinements against the template structures PDB entries 193l (Vaney *et al.*, 1996) and 9ins (Gursky *et al.*, 1992), respectively. The structures obtained from molecular replacement using the *Auto-Rickshaw* web server (Panjikar *et al.*, 2005, 2009) were further refined using *PHENIX* (Adams *et al.*, 2010) and manually checked with *Coot* (Emsley *et al.*, 2010). The final crystal structures were deposited in the PDB (HPF tHEWL, PDB entry 4a7d; HPF cubic insulin, PDB entry 4a7e). Refinement statistics are summarized in Table 4. No structural changes could be observed compared with structures obtained from conventionally flash-cooled crystals.

3. Results and discussion

3.1. Water vitrification

This work demonstrates the successful HPF of three different proteins including a membrane protein. The crystals are not cryoprotected or oil coated and are directly cooled in their mother liquor. After HPF the samples appeared clear and transparent, indicating homogeneous vitrification. The results obtained from optical sample inspection are consistent for all protein crystals and are in good agreement with the observations made in the diffraction experiments. Figs. 4 and 5 show representative diffraction images collected from HPF crystals of cubic insulin and PSII, respectively. In the diffraction patterns, no diffraction rings owing to hexagonal ice are visible (Dowell & Rinfret, 1960). This clearly shows that the solvent inside the crystals as well as the surrounding solution could be completely vitrified by HPF without the addition of cryoprotectants by applying a pressure of 210 MPa and rapid cooling.

3.2. Crystal quality

Resolution limit, crystal mosaicity, $\langle I/\sigma(I)\rangle$, R_{merge} and the Wilson B factor were used to evaluate the crystal quality after HPF. Crystal-quality indicators for ten HPF tHEWL and three HPF cubic insulin crystals are given in Table 3. In general, the diffraction quality of the HPF samples is similar to that reported for cryoprotected crystals flash-cooled at ambient pressure (for comparison, see Vaney *et al.*, 1996; Sauter *et al.*, 2001; Nanao *et al.*, 2005; Meents *et al.*, 2007; Yu & Caspar, 1998).

In the case of tHEWL the crystal mosaicities obtained from ten crystals varied between 0.14° and 0.99°. Such differences in crystal mosaicity are also observed for conventionally flash-cooled tHEWL crystals and are therefore probably not a feature of the applied HPF procedure. Depending on the crystallization and cryoprotection conditions, tHEWL crystals typically show crystal mosaicities

between 0.49 and 0.83° when flash-cooled to cryogenic temperatures (Bujacz *et al.*, 2010).

In contrast, the individual crystal-quality parameters of HPF cubic insulin were very consistent. The three HPF cubic insulin crystals showed a small average mosaicity of only 0.09 ± 0.01°, whereas cryoprotected flash-cooled crystals of cubic insulin typically exhibit mosaicities of 0.14° (Meents *et al.*, 2007).

The structure refinements revealed that the structural perturbations induced by the rapid pressurization (20 ms) and cooling (7000 K s^{-1}) applied in this work are comparable with those which typically arise upon conventional flash-cooling at ambient pressure or slow cooling (1–2 K s^{-1}) at high pressures. For HPF structure 4a7e the positions of 55 water molecules could be refined. This is comparable to the number of water molecules refined for other low-temperature cubic porcine insulin structures obtained from conventionally flash-cooled crystals, such as PDB entry 2g4m, which contains 61 water molecules (Mueller-Dieckmann *et al.*, 2007).

The HPF PSII crystal diffracted to a resolution of 4.5 Å, which is lower than the resolution recently reported for cryoprotected PSII crystals flash-cooled at ambient pressure (Umena *et al.*, 2011; Guskov *et al.*, 2009). This is probably a result of the different crystallization protocol and the smaller crystal size in our approach. For the first 10° of the HPF PSII data a crystal mosaicity of 0.22° was obtained, which then increases, probably as a consequence of radiation damage. The diffraction pattern of the HPF PSII crystal shown in Fig. 5 is highly anisotropic. This means that the attained resolution and the calculated mosaicity depend on the orientation of the crystal in the X-ray beam. Such strongly anisotropic diffraction has also been observed for glycerol-cryoprotected PSII crystals (Kern, Loll, Zouni *et al.*, 2005). Thus, this feature seems to originate from the packing of the dimeric PSII complexes in the unit cell rather than being induced by the HPF procedure.

Owing to the relatively low crystal symmetry and the sample holder, it was not possible to collect complete diffraction data from PSII. In the present setup the HPF PSII crystal is mounted on the beamline together with the Teflon ring. This results in an overall sample diameter of 3 mm, which might cause turbulence in the cryostream. The Teflon ring has a wall thickness of 0.5 mm and caused some additional background scatter on the detector. In the future, it is intended to remove the Teflon ring from the sample. This should allow optimal sample cooling and the collection of full rotation data sets, which is especially important for low-symmetry crystals.

4. Conclusion and outlook

In contrast to other HPF procedures published to date in the field of macromolecular cryocrystallography (see Table 1), our technique allows the rapid cooling of macromolecular crystals in their mother liquor without any cryoprotectants or external reagents, such as oils. In the present work, protein crystals were subjected to HPF using a commercially available device. The Baltec HPM 010 instrument is part of the standard equipment in biological EM laboratories and is therefore accessible to a wide range of users. The HPM 010 machine provides rapid pressurization (20 ms) and rapid cooling rates (7000 K s^{-1}) at the sample surface. This allows vitrification of the solvent inside the crystal and of the surrounding solution without the formation of hexagonal ice. The HPF method presented here is very flexible and allows the cryocooling of many different types of samples without removing the crystal from the mother liquor. Method *A* is especially suited to crystals which can be directly grown in quartz capillaries. Method *B* allows HPF of crystals in a drop of crystallization solution without the use of quartz capillaries. The protein crystals can be grown by any crystallization technique, such as hanging-drop vapour diffusion or dialysis.

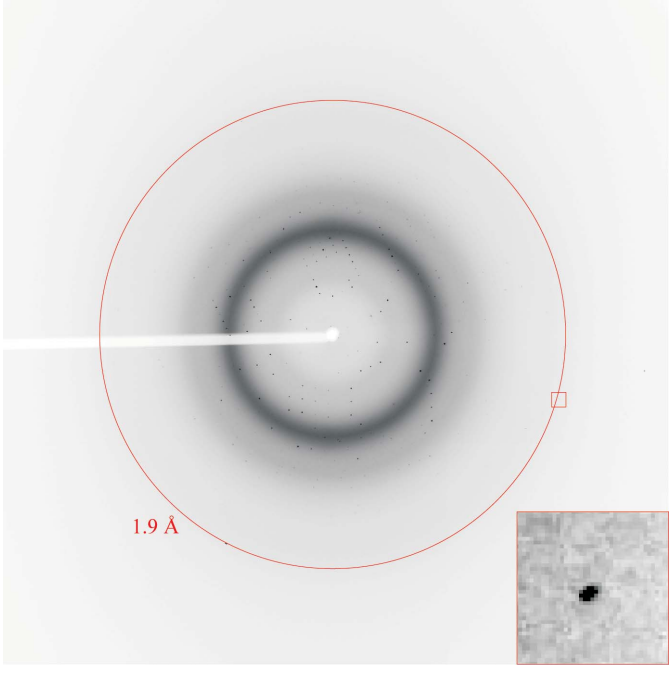

Figure 4
Diffraction image of an HPF cubic insulin crystal collected at beamline X06DA at the Swiss Light Source. The red ring indicates a resolution of 1.9 Å. An enlarged picture of the boxed area showing Bragg reflections at 1.9 Å resolution is shown at the bottom right.

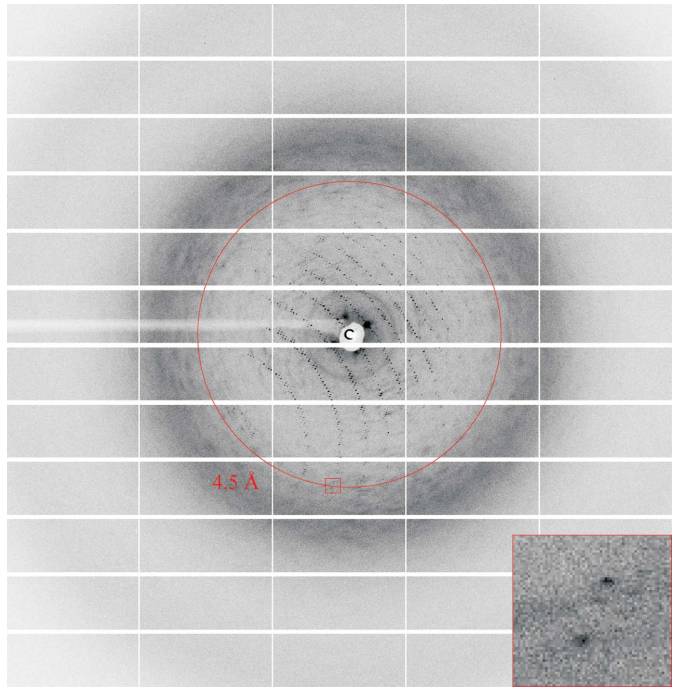

Figure 5
Diffraction image of an HPF crystal of PSII collected at beamline I24 at Diamond Light Source. The red ring indicates a resolution of 4.5 Å. An enlarged picture of the boxed area showing Bragg reflections at 4.5 Å resolution is shown at the bottom right.

Our method eliminates the time-consuming search for suitable cryoconditions. This is of special importance for macromolecules that are too scarce to allow such optimization.

The diffraction quality of the HPF crystals is similar to that of cryoprotected flash-cooled crystals. In the case of cubic insulin, an excellent crystal mosaicity of 0.09° was achieved. The method is therefore very well suited to cryocooling large-unit-cell systems where overlap of reflections owing to the high mosaicity caused by the cooling procedure becomes a problem. Our results show that HPF applying rapid cooling rates is a very attractive alternative for macromolecules for which flash-cooling using conventional methods is problematic or even impossible, such as viruses or membrane proteins. Initial HPF experiments on a crystal of the membrane protein PSII gave very promising results. For the first time, a membrane protein could be successfully cooled without the addition of any cryoprotectants. The PSII crystal diffracted to a resolution of 4.5 Å after HPF. This shows that our HPF protocol is applicable to the cryocooling of sensitive crystal lattices and large-unit-cell systems with weak crystal contacts. Further HPF experiments on such delicate samples are currently in progress and will be the main focus of our future HPF studies.

This work was supported by SLS Proposal 20110059 'High Pressure Freezing of Macromolecular Crystals'. The authors would like to thank J. Brandao-Neto, A. Douangamath, D. Axford, E. Panepucci and S. Waltersperger for technical support during the diffraction experiments. The work on PSII was supported by the DFG Cluster of Excellence 'Unifying Concepts in Catalysis' (project B1) coordinated by Technical University Berlin. Illustrations of the HPF setup were kindly provided by M. Holthaus.

References

Adams, P. D. *et al.* (2010). *Acta Cryst.* D**66**, 213–221.
Bald, W. B. (1986). *J. Microsc.* **143**, 89–102.
Barstow, B., Ando, N., Kim, C. U. & Gruner, S. M. (2008). *Proc. Natl Acad. Sci. USA*, **105**, 13362–13366.
Bujacz, G., Wrzesniewska, B. & Bujacz, A. (2010). *Acta Cryst.* D**66**, 789–796.
Chen, Y.-F., Tate, M. W. & Gruner, S. M. (2009). *J. Appl. Cryst.* **42**, 525–530.
Dahl, R. & Staehelin, L. A. (1989). *J. Electron Microsc. Tech.* **13**, 165–174.
Domsic, J. F., Avvaru, B. S., Kim, C. U., Gruner, S. M., Agbandje-McKenna, M., Silverman, D. N. & McKenna, R. (2008). *J. Biol. Chem.* **283**, 30766–30771.
Dorfmüller, T., Hering, W. T. & Stierstadt, K. (1998). *Lehrbuch der Experimentalphysik: Mechanik, Relativität, Wärme*, edited by L. Bergmann & C. Schaefer, p. 418. Berlin: de Gruyter.
Dowell, L. G. & Rinfret, A. P. (1960). *Nature (London)*, **188**, 1144–1148.
Emsley, P., Lohkamp, B., Scott, W. G. & Cowtan, K. (2010). *Acta Cryst.* D**66**, 486–501.
Englich, U., Kriksunov, I. A., Cerione, R. A., Cook, M. J., Gillilan, R., Gruner, S. M., Huang, Q., Kim, C. U., Miller, W., Nielsen, S., Schuller, D., Smith, S. & Szebenyi, D. M. E. (2011). *J. Synchrotron Rad.* **18**, 70–73.
Fry, E. E., Abrescia, N. G. A. & Stuart, D. I. (2007). *Macromolecular Crystallography: Conventional and High-Throughput Methods*, edited by M. R. Sanderson & J. V. Skelly, pp. 245–263. Oxford University Press.
García-Ruiz, J. M. & Moreno, A. (1994). *Acta Cryst.* D**50**, 484–490.
Garman, E. F. & Owen, R. L. (2006). *Acta Cryst.* D**62**, 32–47.
Garman, E. F. & Schneider, T. R. (1997). *J. Appl. Cryst.* **30**, 211–237.
Gursky, O., Li, Y., Badger, J. & Caspar, D. L. (1992). *Biophys. J.* **61**, 604–611.
Guskov, A., Kern, J., Gabdulkhakov, A., Broser, M., Zouni, A. & Saenger, W. (2009). *Nature Struct. Mol. Biol.* **16**, 334–342.
Hohenberg, H., Mannweiler, K. & Müller, M. (1994). *J. Microsc.* **175**, 34–43.
Kabsch, W. (2010). *Acta Cryst.* D**66**, 125–132.
Kern, J., Loll, B., Lüneberg, C., DiFiore, D., Biesiadka, J., Irrgang, K.-D. & Zouni, A. (2005). *Biochim. Biophys. Acta*, **1706**, 147–157.
Kern, J., Loll, B., Zouni, A., Saenger, W., Irrgang, K.-D. & Biesiadka, J. (2005). *Photosynth. Res.* **84**, 153–159.
Kim, C. U., Hao, Q. & Gruner, S. M. (2006). *Acta Cryst.* D**62**, 687–694.
Kim, C. U., Kapfer, R. & Gruner, S. M. (2005). *Acta Cryst.* D**61**, 881–890.
Meents, A., Gutmann, S., Wagner, A. & Schulze-Briese, C. (2010). *Proc. Natl Acad. Sci. USA*, **107**, 1094–1099.
Meents, A., Wagner, A., Schneider, R., Pradervand, C., Pohl, E. & Schulze-Briese, C. (2007). *Acta Cryst.* D**63**, 302–309.
Moor, H. (1971). *Philos. Trans. R. Soc. Lond. B Biol. Sci.* **261**, 121–131.
Mueller-Dieckmann, C., Panjikar, S., Schmidt, A., Mueller, S., Kuper, J., Geerlof, A., Wilmanns, M., Singh, R. K., Tucker, P. A. & Weiss, M. S. (2007). *Acta Cryst.* D**63**, 366–380.
Nanao, M. H., Sheldrick, G. M. & Ravelli, R. B. G. (2005). *Acta Cryst.* D**61**, 1227–1237.
Otálora, F., García-Ruiz, J. M. & Moreno, A. (1996). *J. Cryst. Growth*, **168**, 93–98.
Panjikar, S., Parthasarathy, V., Lamzin, V. S., Weiss, M. S. & Tucker, P. A. (2005). *Acta Cryst.* D**61**, 449–457.
Panjikar, S., Parthasarathy, V., Lamzin, V. S., Weiss, M. S. & Tucker, P. A. (2009). *Acta Cryst.* D**65**, 1089–1097.
Riehle, U. (1968). *Chem. Ing. Tech.* **40**, 213–218.
Rodgers, D. W. (1994). *Structure*, **2**, 1135–1140.
Sauter, C., Otálora, F., Gavira, J.-A., Vidal, O., Giegé, R. & García-Ruiz, J. M. (2001). *Acta Cryst.* D**57**, 1119–1126.
Sheldrick, G. M., Dauter, Z., Wilson, K. S., Hope, H. & Sieker, L. C. (1993). *Acta Cryst.* D**49**, 18–23.
Shimoni, E. & Müller, M. (1998). *J. Microsc.* **192**, 236–247.
Studer, D., Humbel, B. M. & Chiquet, M. (2008). *Histochem. Cell Biol.* **130**, 877–889.
Studer, D., Michel, M., Wohlwend, M., Hunziker, E. B. & Buschmann, M. D. (1995). *J. Microsc.* **179**, 321–332.
Thomanek, U. F., Parak, F., Mössbauer, R. L., Formanek, H., Schwager, P. & Hoppe, W. (1973). *Acta Cryst.* A**29**, 263–265.
Umena, Y., Kawakami, K., Shen, J.-R. & Kamiya, N. (2011). *Nature (London)*, **473**, 55–60.
Urayama, P., Phillips, G. N. & Gruner, S. M. (2002). *Structure*, **10**, 51–60.
Vaney, M. C., Maignan, S., Riès-Kautt, M. & Ducruix, A. (1996). *Acta Cryst.* D**52**, 505–517.
Yu, B. & Caspar, D. L. (1998). *Biophys. J.* **74**, 616–622.